

Electronic Supplementary Information

Mesoporous carbon material co-doped with nitrogen and iron (Fe-N-C): Highly performing cathode catalyst for oxygen reduction reaction in alkaline electrolyte

Xiang-Hui Yan, and Bo-Qing Xu*

Innovative Catalysis Program, Key Lab of Organic Optoelectronics & Molecular Engineering,
Department of Chemistry, Tsinghua University, Beijing, 100084, China

*Corresponding author. Tel.: (+86)10-6279-2122

E-mail: bqxu@mail.tsinghua.edu.cn

Experimental detail

Catalyst synthesis: SBA-15 was fabricated according to the literature.¹ The mesoporous Fe-N-C catalysts were prepared according to a modified methodology reported in literature (scheme S1).^{2,3} In typical synthesis, 2.0 mL of aniline was dispersed in 0.5 M HCl solution containing 0.4 g SBA-15. The suspension was stirred for 2 h below 10 °C followed by addition of 1 M ammonium peroxydisulfate (APS) and a required amount of ferric chloride hexahydrate. After stirring for 24 h, the mixture was dried at 100 °C for overnight. The resultant dark green colored composite was ground into a fine powder and carbonized in nitrogen gas with a heating rate of 5.0 °C min⁻¹ to 900 °C and then kept for one hour and finally cooled to room temperature (HT1). To dissolve the silica template SBA-15, the carbonized sample was etched in 2 M NaOH at 60 °C for 24 h, washed with de-ionized water and ethanol, and then dried at 100 °C for overnight (DS). The etched sample was heat-treated again for 3 h under identical conditions to the first heat treatment (HT2). The sample obtained at the termination of the second heat-treatment (HT2) was denoted as PANI-xFe-HT2(SBA-15) (x refers to the final Fe content in wt%). For comparisons, three other samples were also prepared under the identical conditions except without the addition of SBA-15, FeCl₃ and both of them, respectively, denoting PANI-xFe-HT2, PANI-HT2(SBA-15) and PANI-HT2, respectively.

Characterization: TEM images were taken using JEOL JEM-2010 microscope equipped with EDX detector operated at 120 kV. The X-ray powder diffraction patterns were recorded on a D-Max-2200PC diffractometer using Cu K α radiation ($\lambda = 1.5418 \text{ \AA}$) at 40 kV and 30 mA at a scan rate of 0.5° min⁻¹ for small angle and 5° min⁻¹ for wide angle. X-ray photoelectron spectroscopy (XPS) measurements were carried out on an EscaLab 250Xi spectrometer equipped with monochromatic Al K α X-ray source (1253.6 eV) and the calibration of binding energy (BE) of the spectra

was referenced to the C1s electron bonding energy at 284.6 eV. The N₂ adsorption-desorption isotherms were obtained at 77 K using a Micromeritics ASAP 2010 instrument. Prior to the measurement, the samples were outgassed at 473 K under vacuum. BET and BJH analyses were used to determine the surface area, pore size distribution, and pore volume. After the PANI-xFe-HT2 and PANI-xFe-HT2(SBA-15) were treated in air by temperature-programmed oxidation (TPO) measurements, the resulted thermal residues were dissolved in aqua regia and then diluted with deionized water. The iron concentrations in the dilute solution were determined by inductively coupled plasma-atomic emission spectroscopy (ICP-AES) using a Perkin Elmer Optima 3300 RL instrument.

Electrode preparation: Prior to the preparation of the working electrode, the blank electrode was carefully polished on a polishing cloth using 0.5 and then 0.05 μm alumina slurry, followed by washing ultrasonically with HNO₃ (1 : 1), ethanol, acetone and then deionized water. The catalyst ink was prepared by dispersing 3 mg PANI-derived samples in 0.5 mL mixture of Nafion (5 wt%) and deionized water (1/9, V/V) under sonication. 20 μL of the obtained catalyst ink was transferred onto the polished electrode with a loading of 0.61 mg cm⁻² until solvent evaporation. This loading amount was previously used by Zelenay et al.^{2,3} in their earlier studies on Fe-N-C catalysts for ORR in acidic electrolyte. For comparison, 20 wt% E-TEK Pt/C catalyst ink was also prepared as the same procedure described above and then transferred onto the polished electrode with a Pt loading of 20 μg_{Pt} cm⁻², the global loading of Pt/C was 102 $\mu\text{g}\cdot\text{cm}^{-2}$.

Electrochemical Measurements: All Electrochemical measurements, including cyclic voltammetry (CV), linear sweep voltammetry (LSV) and chronoamperometry (CA) were performed at room temperature in a three-electrode cell using a potentiostat/galvanostat Model 263A (PAR). A glassy carbon rotating disk electrode

(GC-RDE, 0.19625 cm²) was employed as the working electrode. Ag/AgCl (in 3.5 M KCl) and a Pt wire were used as the reference and counter electrodes, respectively. Prior to each measurement for ORR, the working electrode coated with catalyst was pretreated by CV in N₂-saturated 0.1 M KOH electrolyte for at least 30 cycles until the electrode surface was electrochemical stable. The electrolyte was then purged with high purity oxygen until saturation. Afterwards, the ORR measurements were conducted and a gentle oxygen flow was kept during the whole measurement. The CVs were first recorded at a scanning rate of 100 mV s⁻¹ from -1.0 to 0.2 V vs Ag/AgCl until the last two cycles overlapped and polarization curves were then recorded at a scanning rate of 10 mV s⁻¹ with various rotation rates from 600 to 2200 rpm. ORR currents from polarization curves were normalized in reference to the geometric area of the GC-RDE and subtracted the background currents, which was obtained by conducting the voltammetry under N₂-saturated 0.1 M KOH.

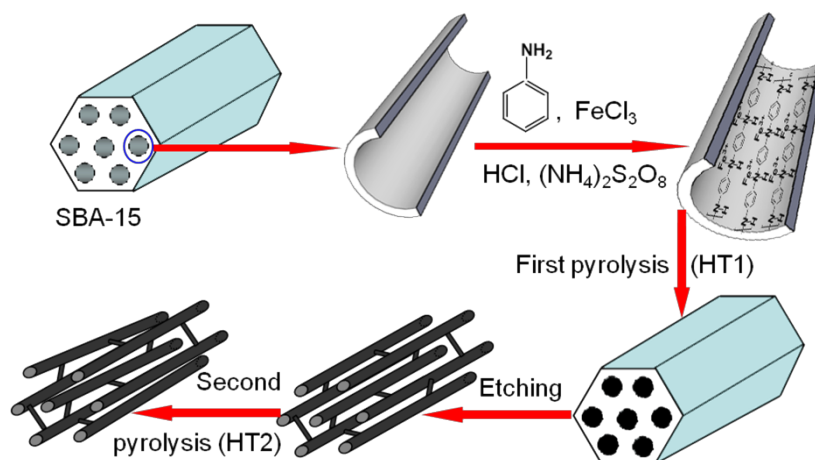
The number of transferred electrons and kinetic current density in the ORR can be calculated from Koutecky-Levich (K-L) equation:^{4,5}

$$(1) J^{-1} = J_L^{-1} + J_k^{-1} = (B\omega^{1/2})^{-1} + J_k^{-1}$$

$$(2) B = 0.20 nFC_0(D_0)^{2/3}v^{-1/6}$$

$$(3) J_k = nFkC_0$$

where J is the measured current density, J_L and J_k is the diffusion-limiting and kinetic current density, ω is the electrode rotation speed (rpm), n is the number of transferred electrons required on the average for the reduction of an oxygen molecule, F is the Faraday constant ($F = 96485 \text{ C mol}^{-1}$), C_0 and D_0 are the bulk concentration and diffusion coefficient of O₂ ($C_0 = 1.2 \times 10^{-3} \text{ mol/L}$, $D_0 = 1.9 \times 10^{-5} \text{ cm}^2 \text{ s}^{-1}$), respectively, v is the kinematic viscosity of the electrolyte ($v = 0.01 \text{ cm}^2 \text{ s}^{-1}$), and k is the electron-transfer rate constant. According to equations (1) and (2), the n and J_k can be obtained from the slope and intercept of the Koutecky-Levich plots, respectively.



Scheme S1. Procedure for the synthesis of ordered mesoporous Fe-N-C catalyst.

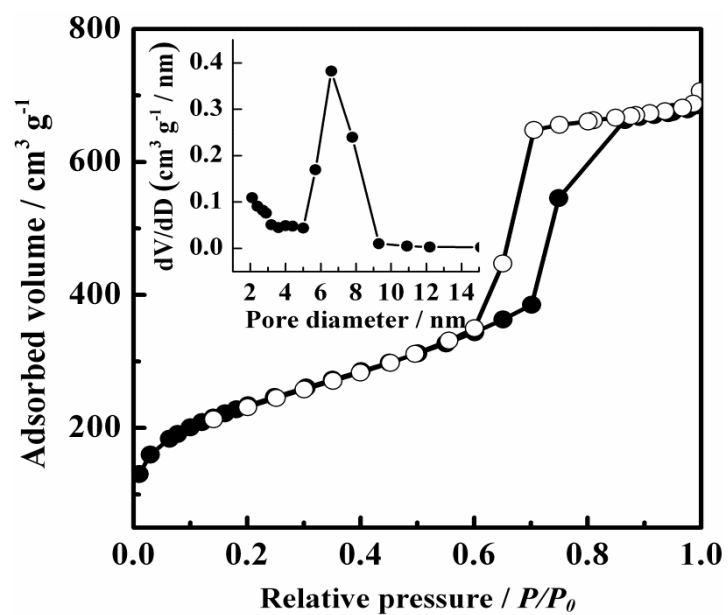


Fig. S1. N_2 adsorption/desorption isotherms and pore size distribution of the SBA-15 template.

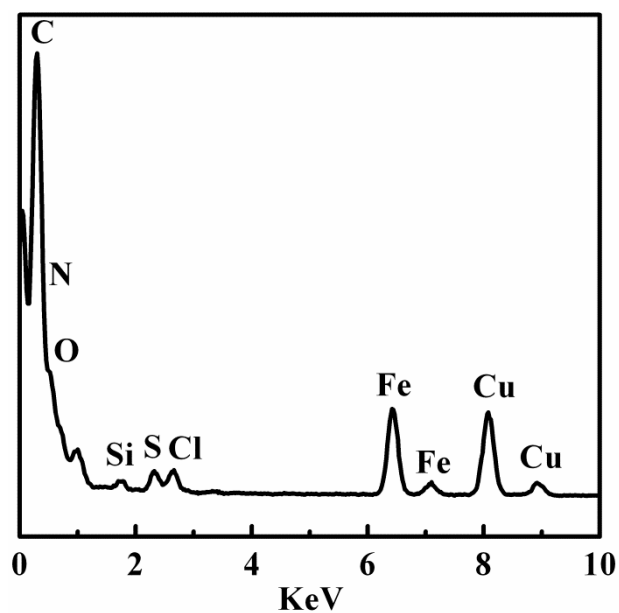


Fig. S2. EDX spectrum of PANI-4.5Fe-HT2(SBA-15).

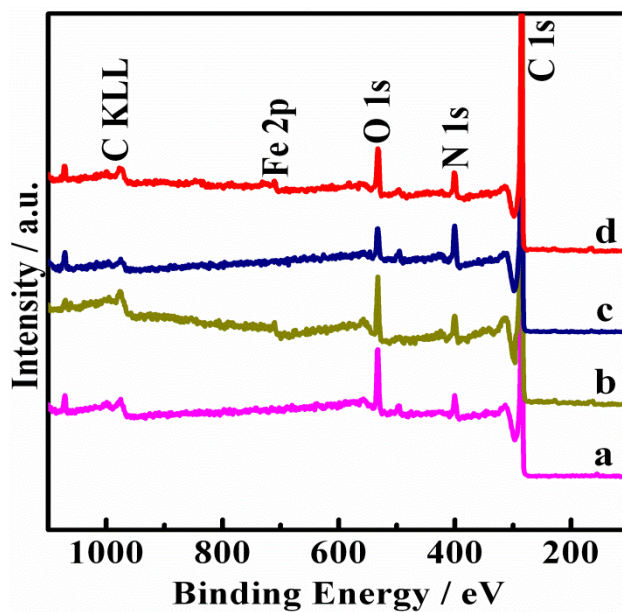


Fig. S3. XPS survey spectra of the PANI-HT2 (a), PANI-4.5Fe-HT2 (b), PANI-HT2(SBA-15) (c) and PANI-4.5Fe-HT2(SBA-15) (d).

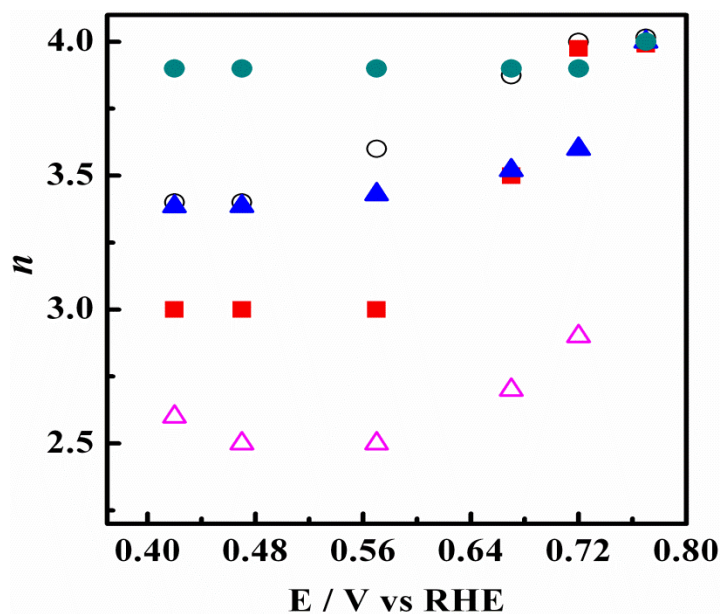


Fig. S4. Number of transferred electrons (n) per O_2 -reduction at varied potentials on PANI-HT2 (Δ), PANI-4.5Fe-HT2 (\circ), PANI-HT2(SBA-15) (\blacksquare), PANI-4.5Fe-HT2(SBA-15) (\blacktriangle) and Pt/C catalyst (\bullet) at varied potentials.

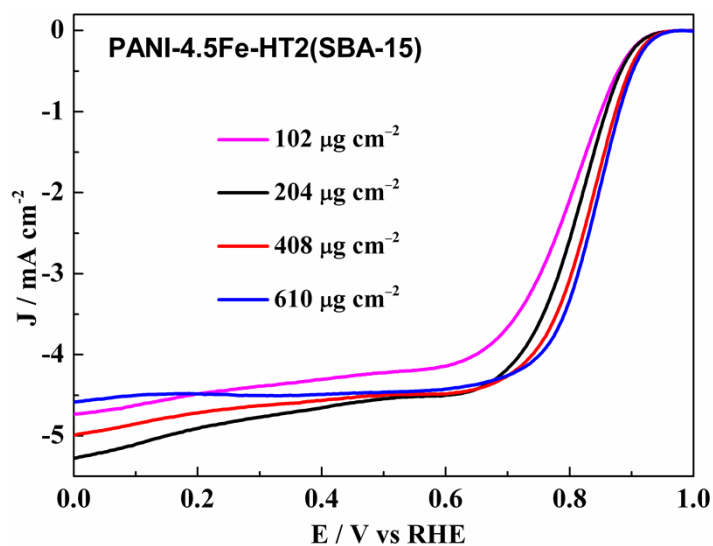


Figure S5 Effect of catalyst loading on the ORR polarization curve of PANI-4.5Fe-HT2 (SBA-15). Measurement conditions: temp.: 25 °C, electrolyte: 0.1 M KOH, scan rate: 10 mV s⁻¹, electrode rotation-speed: 1600 rpm.

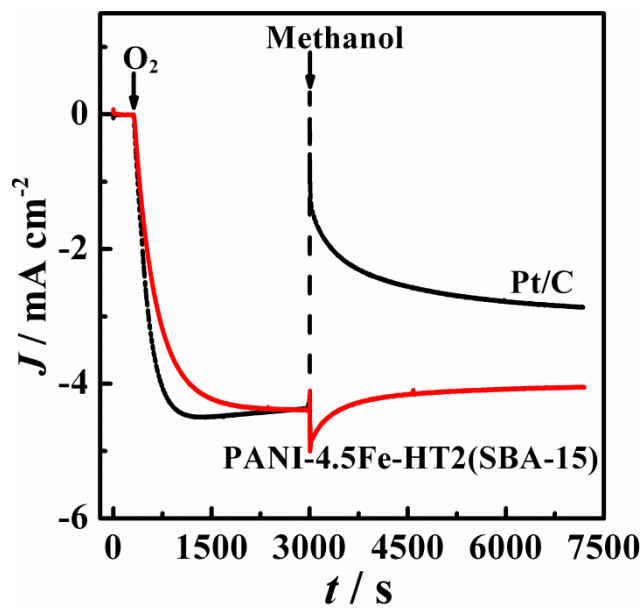


Fig. S6. Chronoamperometric evaluations for resistance to methanol oxidation of PANI-4.5Fe-HT2(SBA-15) and Pt/C catalysts at 0.57 V in O_2 -saturated 0.1 M KOH electrolyte. The RDE rotation speed was 1600 rpm and the concentration of methanol added was made 3 M in the electrolyte.

Table S1. Textural properties, overall nitrogen content and chemical identities of nitrogen species of the PANI-derived samples.*

Sample	S_{BET} ($\text{m}^2 \text{g}^{-1}$)	V ($\text{cm}^3 \text{g}^{-1}$)	D_p (nm)	N (at.%)	Percentage of doped-N in various N-species (%)			
					N_1	N_2	N_3	N_4
PANI-HT2	51	0.11	< 2	4.9	34.5	0	65.5	0
PANI-4.5Fe-HT2	58	0.16	< 2	4.6	23.6	10.5	59.5	6.3
PANI-HT2(SBA-15)	297	0.40	4.0	8.3	18.8	5.4	69.8	5.9
PANI-4.5Fe-HT2(SBA-15)	236	0.27	3.9	7.6	18.8	15.5	56.2	9.3

* S_{BET} : BET specific surface area; V : pore volume; D_p : the most probable pore size from the desorption branches. N : overall nitrogen content determined by XPS elemental analysis. N_1 , N_2 , N_3 and N_4 denote pyridinic N, pyrrolic N, quaternary N and pyridinic $\text{N}^+\text{-O}$, respectively.

Table S2. Surface chemical composition and atomic concentration of the PANI-derived samples.*

Sample	C	O	Fe	N				S	Si	Cl
				N_1	N_2	N_3	N_4			
PANI-HT2	86.59	8.31	0	1.71	0	3.25	0	0.10	0	0.04
PANI-4.5Fe-HT2	87.53	7.12	0.30	1.08	0.48	2.72	0.29	0.44	0	0.05
PANI-HT2(SBA-15)	87.04	4.33	0	1.56	0.45	5.78	0.49	0.17	0.11	0.07
PANI-4.5Fe-HT2(SBA-15)	82.63	8.16	0.44	1.43	1.18	4.27	0.71	0.66	0.45	0.07

* Determined by XPS elemental analysis and the atomic concentration was given with respect to at.%. See the footnote of **Table S1** for the meanings of N_1 , N_2 , N_3 and N_4 .

Table S4. Comparison of the ORR activity on the PANI-4.5Fe-HT2(SBA-15) in 0.1 M KOH with that of various NPMCs in literature.^a

Catalyst	Loading ($\mu\text{g}/\text{cm}^2$)	E_{onset} (V)	$E_{1/2}$ (V)	J_k (mA cm^{-2}) (0.82 V)	Ref.
G-CN800	71	0.87	0.74	0.4	6
P-doped graphite	102	0.82	0.65	0.3	7
CNT/HDC-1000	605	0.92	0.82	4.6	8
I-doped graphene	28	0.90	n.a ^b	1.7	9
B-doped graphene	142	0.88	n.a	0.2	10
N-doped carbon nanocapsules	1714	0.89	0.70	0.9	11
N-doped Carbon	379	0.92	0.76	2.0	12
N-doped graphene	51	0.97	0.79	3.0	13
N-doped Graphene/Fe _{5.0}	51	0.96	0.75	1.5	13
PDMC-800	100	0.81	0.69	0	14
Graphitic C ₃ N ₄ /Carbon	85	0.84	0.67	0.4	15
P-doped ordered mesoporous carbon	159	0.88	0.77	1.5	16
Carbon nanotube-Graphene	485	0.92	0.76	1.7	17
Fe-N _{70%} /C-800	276	0.91	0.79	1.8	18
S-N-CF-1000	142	1.00	0.80	4.9	19
HP-Co-CN-900	n.a.	0.87	0.77	0.9	20
PANI-4.5Fe-HT2(SBA-15)	102	0.95	0.80	2.71	This work.
	204	0.95	0.81	3.7	This work
	408	0.95	0.83	5.9	This work
	610	0.95	0.84	7.4	This work

^a E_{onset} and $E_{1/2}$ were estimated from the polarization curves at 1600 rpm given in the literature.⁶⁻²⁰

The “-” refers to that $E_{1/2}$ could not be read due to the diffusion-limiting current density not being obtained. The J_k values in literature [6–16] are estimated from the polarization curves at 1600 rpm according to equation of $1/J_k = 1/J - 1/J_L$. All potentials were given with respect to RHE, according to Nernst equation which is simplified to $E(\text{RHE}) = E(\text{Ag/AgCl}) + 0.2046 \text{ V} + 0.059 \text{ pH}$ (pH = 13 for 0.1 M KOH). ^b Not available in the original paper.

References

- 1 D. Y. Zhao, Q. S. Huo, J. L. Feng, B. F. Chmelka and G. D. Stucky, *J. Am. Chem. Soc.*, 1998, **120**, 6024.
- 2 G. Wu, C. M. Johnston and P. Zelenay, *J. Mater. Chem.*, 2011, **21**, 11392.
- 3 G. Wu, K. L. More, C. M. Johnston and P. Zelenay, *Science*, 2011, **332**, 443.
- 4 A. J. Bard and L. R. Faulkner, *Electrochemical Methods: Fundamentals and Applications*, John Wiley & Sons, New York, 2nd edn., 2001, ch. 9, pp. 339-343. chapter 8.
- 5 G. R. Zhang and B. Q. Xu, *Chin. J. Catal.*, 2013, **34**, 942.
- 6 S. B. Yang, X. L. Feng, X. C. Wang and K. Müllen, *Angew. Chem. Int. Ed.*, 2011, **50**, 5339.
- 7 Z. W. Liu, F. Peng, H. J. Wang, H. Yu, W. X. Zheng and J. Yang, *Angew. Chem. Int. Ed.*, 2011, **50**, 3257.
- 8 J. Sa, C. Park, H. Y. Jeong, S.-H. Park, Z. Lee, K. T. Kim, G.-G. Park and S. H. Joo, *Angew. Chem. Int. Ed.*, 2014, **53**, 1.
- 9 Z. Yao, H. G. Nie, Z. Yang, X. M. Zhou, Z. Liu and S. M. Huang, *Chem. Comm.*, 2012, **48**, 1027.
- 10 Z. H. Sheng, H. L. Gao, W. J. Bao, F. B. Wang and X. H. Xia, *J. Mater. Chem.*, 2012, **22**, 390.
- 11 S. Shanmugam and T. Osaka, *Chem. Comm.*, 2011, **47**, 4463.
- 12 H. X. Zhong, H. M. Zhang, Z. Xu, Y. F. Tang and J. X. Mao, *ChemSusChem*, 2012, **5**, 1698.
- 13 K. Parvez, S. B Yang, Y. Hernandez, A. Winter, A. Turchanin, X. L. Feng and K. Müllen, *ACS Nano*, 2012, **6**, 9841.
- 14 R. Silva, D. A. Voiry, M. Chhowalla and T. Asefa, *J. Am. Chem. Soc.*, 2013, **135**, 7823.
- 15 J. Liang, Y. Zheng, J. Chen, J. Liu, D. Hulicova-Jurcakova, M. Jaroniec and S. Z. Qiao, *Angew. Chem. Int. Ed.*, 2012, **51**, 1.
- 16 D. S. Yang, D. Bhattacharjya, S. Inamdar, J. Park and J. S. Yu, *J. Am. Chem. Soc.*, 2012, **134**, 16127.
- 17 Y. G. Li, W. Zhou, H. L. Wang¹, L. M. Xie, Y. Y. Liang, F. Wei, J. C. Idrobo, S. J. Pennycook and H. J. Dai, *Nature Nanotech.*, 2012, **7**, 394.
- 18 Q. Cui, L. S. J. Chao, P. H. Wang, Z. Y. Bai, H. Yan, K. Wang and L. Yang, *RSC Adv.*, DOI: 10.1039/C3RA44958K
- 19 Z. Liu, H. G. Nie, Z. Yang, J. Zhang, Z. P. Jin, Y. Q. Lu, Z. B. Xiao and S. M. Huang, *Nanoscale*, 2013, **5**, 3283.
- 20 H. L. Jiang, Y. H. Su, Y. H. Zhu, J. H. Shen, X. L. Yang, Q. Feng and C. Z. Li, *J. Mater. Chem. A*, 2013, **1**, 12074.